Dynamics of the elements of the printing device

K. Ragulskis[1], E. Kibirkštis[1], A. Bubulis[1], L. Zubavičius[2], R. Maskeliūnas[2], L. Ragulskis[3]

[1]*Kaunas University of Technology*

[2]*Vilnius Gediminas Technical University*

[3]*Vytautas Magnus University*

Introduction

The schematic diagrams of the printing machine and its elements are presented in [1]. One of the basic components of the printing machine is the printing cylinder. Various types of vibration and wave motions can take place in it. In this paper longitudinal waves in the printing cylinder are analyzed. They are understood as longitudinal from the point of view of the whole cylinder and its axis of symmetry. From the point of view of the surface element of the cylinder they are usually flexural. Another important problem in the analysis of the printing devices is investigation of the dynamics of the printing ink as a viscous fluid.

The dynamics of an axisymmetric composite shell problem is analyzed in this paper. The axisymmetric shell is considered to have two external layers of higher stiffness and an internal layer of lower stiffness. The finite element of this axisymmetric shell problem is obtained from the contributions of the three sub-elements. The resulting finite element has six degrees of freedom per node. The eigenmodes are calculated and it is evident that the multiple eigenmodes enable the excitation of wave motion in this system. The analysis is based on [2, 3].

The problem of fluid flow control exploiting the vibrations of a flow boundary is important in the process of design of various engineering devices and optimization of processes of conveyance [10, 9, 7, 6]. Analysis of such a dynamical system requires development of adequate mathematical models and appropriate strategies for numerical modeling [11, 14, 5, 4].

One of the specific precision engineering applications where vibrations play a key role in controlling a fluid flow is dosing and spraying of liquid materials. Particular interest exists for elastic catheter pipe type dosing equipment [9, 7, 12] where the application of piezoelectric actuators for the generation of standing waves in the outlet pipe can produce effects which can be used for the control of dosing process.

Definite attention exists for the analysis of tube vibrations induced by internal or external flow [8]. Analysis of such vibrations is very important in many engineering applications including nano-tube vibrations.

Nevertheless, analysis of an inverse problem – flow control by forced longitudinal and transverse vibrations of the tube itself is also of interest. Such a vibration based flow control methodology builds ground for the development of new types of liquid material dosing equipment. It is understood that full analysis of such complex problems requires construction of three dimensional models, but the analysis of such models and the interpretations of those results would be quite complicated.

A two dimensional model is developed in this paper. The external excitation of the boundary by longitudinal vibrations is encountered through the boundary conditions of the flow of non-Newtonian fluid. Flow excitation by transverse vibrations of the tube is represented through the convective acceleration terms in the equation of dynamic equilibrium of the fluid flow in the cross section of the tube. The excitation velocities are assumed to be equal in the whole cross section area and are the functions of time only. The obtained results provide insight into the process of vibration based control of fluid flow. It is assumed that the boundary (the tube) is a non-deformable rigid body. A FEM model leads to the first order matrix differential equation. The approximate solution is sought using the modal decomposition and numerical integration of the one-dimensional equations in the time domain. The developed procedure is applicable to tubes of various cross sections and the calculations can be effectively carried out for the required values of the parameters.

The steady state two dimensional viscous incompressible slow flow is analysed. The element of the type described in [3] is used with the nodal variables being the velocity in the direction of the x axis and the velocity in the direction of the y axis and with the incompressibility condition introduced by the penalty method. The photo-elastic analysis produces the intensity proportional to the intensity of the shear strain rate. For such problems in order to obtain acceptable strain rates conjugate approximation with eigen-smoothing is proposed. It is based on the approximation of each of the components of the strain rates by the first eigenmodes of the supplementary problem.

Numerical model of the sub-element of the axi-symmetric shell problem

The sub-element is a modification of the axi-symmetric element for the elastic body presented in [2, 3].

The nodal variables are the tangential displacement of the lower surface of the elastic layer u_1, the transverse displacement of the lower surface of the elastic layer v_1, the tangential displacement of the upper surface of the elastic layer u_2, the transverse displacement of the upper surface of the elastic layer v_2.

Then:

$$\begin{Bmatrix} u \\ v \end{Bmatrix} = \begin{Bmatrix} r_x \\ r_y \end{Bmatrix} u_i + \begin{Bmatrix} t_x \\ t_y \end{Bmatrix} v_i, \tag{1}$$

where u and v are the displacements in the directions of the x and y axes of the orthogonal Cartesian system of co-ordinates for the lower surface of the layer when i=1 and for the upper surface of the layer when i=2, r_x and r_y are the components of the unit tangential vector of the composite shell, t_x and t_y are the components of the unit normal vector of the composite shell, here:

$$\begin{Bmatrix} t_x \\ t_y \end{Bmatrix} = \begin{Bmatrix} -r_y \\ r_x \end{Bmatrix}. \tag{2}$$

At the points of numerical integration of the finite element the transformation to the local directions is performed by the following matrix:

$$[T] = \begin{bmatrix} r_x & r_y \\ t_x & t_y \end{bmatrix} = \begin{bmatrix} \dfrac{dx}{dr} & \dfrac{dy}{dr} \\ -\dfrac{dy}{dr} & \dfrac{dx}{dr} \end{bmatrix}, \tag{3}$$

where r denotes the longitudinal co-ordinate of the axis of the composite shell.

Then:

$$\begin{aligned} \overline{[N_1]} &= \begin{bmatrix} [N_{1u}] \\ [N_{1v}] \end{bmatrix} = \\ &= [T] \begin{bmatrix} \begin{Bmatrix} r_x \\ r_y \end{Bmatrix}_1 N_1 & \begin{Bmatrix} t_x \\ t_y \end{Bmatrix}_1 N_1 & 0 & 0 & \dots \end{bmatrix}, \\ \overline{[N_2]} &= \begin{bmatrix} [N_{2u}] \\ [N_{2v}] \end{bmatrix} = \\ &= [T] \begin{bmatrix} 0 & 0 & \begin{Bmatrix} r_x \\ r_y \end{Bmatrix}_1 N_1 & \begin{Bmatrix} t_x \\ t_y \end{Bmatrix}_1 N_1 & \dots \end{bmatrix}, \end{aligned} \tag{4}$$

where $[N_{1u}]$ and $[N_{1v}]$ are the row vectors for interpolation of the tangential and normal displacements of the lower surface of the layer, $[N_{2u}]$ and $[N_{2v}]$ are the row vectors for interpolation of the tangential and normal displacements of the upper surface of the layer; N_1, … are the shape functions of the finite element; the subscript 1, … after the {} denotes that the corresponding quantities are taken at node 1, ….

The interpolation of the displacements in the transverse direction of the layer is given by:

$$\frac{H-t}{H} \begin{Bmatrix} u_1 \\ v_1 \end{Bmatrix} + \frac{t}{H} \begin{Bmatrix} u_2 \\ v_2 \end{Bmatrix}, \tag{5}$$

where H is the thickness of the layer, $t \in [0, H]$ is the transverse co-ordinate of the layer.

By taking into account that:

$$\begin{aligned} &\int_0^H \frac{H-t}{H} \frac{t}{H} dt = \frac{H}{6}, \\ &\int_0^H \left(\frac{H-t}{H} \right)^2 dt = \int_0^H \left(\frac{t}{H} \right)^2 dt = \frac{H}{3}, \end{aligned} \tag{6}$$

the mass matrix takes the form:

$$[M] = \int \left(\begin{aligned} &\overline{[N_1]}^T \rho \frac{H}{6} \overline{[N_2]} + \\ &+ \overline{[N_2]}^T \rho \frac{H}{6} \overline{[N_1]} + \\ &+ \overline{[N_1]}^T \rho \frac{H}{3} \overline{[N_1]} + \\ &+ \overline{[N_2]}^T \rho \frac{H}{3} \overline{[N_2]} \end{aligned} \right) 2\pi x dr, \tag{7}$$

where ρ is the density of the material of the layer and the value of x is calculated from:

$$x = \sum_i N_i x_i, \tag{8}$$

where x_i are the nodal x coordinates of the middle surface of the composite shell.

The expression for the strains in the layer is given by:

$$\begin{aligned} &\frac{H-t}{H} \begin{Bmatrix} u_{1r} \\ 0 \\ \dfrac{u_1 r_x + v_1 t_x}{x} \\ v_{1r} \end{Bmatrix} + \frac{t}{H} \begin{Bmatrix} u_{2r} \\ 0 \\ \dfrac{u_2 r_x + v_2 t_x}{x} \\ v_{2r} \end{Bmatrix} + \\ &+ \frac{1}{H} \begin{Bmatrix} 0 \\ v_2 - v_1 \\ 0 \\ u_2 - u_1 \end{Bmatrix}, \end{aligned} \tag{9}$$

where the subscript r denotes differentiation in the longitudinal direction of the composite shell and the values of r_x and t_x are determined from Eq 3. So the following matrixes are introduced:

$$\begin{aligned} [B] &= \begin{bmatrix} 0 \\ [N_{2v}] - [N_{1v}] \\ 0 \\ [N_{2u}] - [N_{1u}] \end{bmatrix}, \\ [B_1] &= \begin{bmatrix} [N_{1u}'] \\ 0 \\ \dfrac{[N_{1u}] r_x + [N_{1v}] t_x}{x} \\ [N_{1v}'] \end{bmatrix}, \\ [B_2] &= \begin{bmatrix} [N_{2u}'] \\ 0 \\ \dfrac{[N_{2u}] r_x + [N_{2v}] t_x}{x} \\ [N_{2v}'] \end{bmatrix}, \end{aligned} \tag{10}$$

where the value of x is calculated from Eq. 8, the prime denotes differentiation with respect to the longitudinal axis of the composite shell.

By taking into account that:

$$\begin{aligned} &\int_0^H \frac{H-t}{H} \frac{1}{H} dt = \int_0^H \frac{t}{H} \frac{1}{H} dt = \frac{1}{2}, \\ &\int_0^H \left(\frac{1}{H} \right)^2 dt = \frac{1}{H}, \end{aligned} \tag{11}$$

the stiffness matrix takes the form:

$$[K]=\int\begin{pmatrix}[B]^T[D]\frac{1}{2}[B_1]+[B_1]^T[D]\frac{1}{2}[B]+\\+[B]^T[D]\frac{1}{2}[B_2]+[B_2]^T[D]\frac{1}{2}[B]+\\+[B_1]^T[D]\frac{H}{6}[B_2]+\\+[B_2]^T[D]\frac{H}{6}[B_1]+\\+[B_1]^T[D]\frac{H}{3}[B_1]+\\+[B_2]^T[D]\frac{H}{3}[B_2]+[B]^T[D]\frac{1}{H}[B]\end{pmatrix}2\pi x dr, \quad (12)$$

where:

$$[D]=\begin{bmatrix}K_v+\frac{4}{3}G & K_v-\frac{2}{3}G & K_v-\frac{2}{3}G & 0\\ K_v-\frac{2}{3}G & K_v+\frac{4}{3}G & K_v-\frac{2}{3}G & 0\\ K_v-\frac{2}{3}G & K_v-\frac{2}{3}G & K_v+\frac{4}{3}G & 0\\ 0 & 0 & 0 & \frac{G}{k_s}\end{bmatrix}, \quad (13)$$

where K_v is the modulus of volumetric compressibility of the layer, G is the shear modulus of the layer, k_s is the shear correction factor assumed equal to 1.2 and the value of x is calculated from Eq.8.

Numerical model of the element of the axisymmetric shell problem

The lower and the upper layers are assumed to be stiff and thin. For such a stiff and thin layer the transverse displacements of its lower and upper surfaces are assumed to be mutually equal. The nodal variables are the transverse displacement of the lower layer v_{12}, the tangential displacement of the lower surface of the lower layer u_1, the tangential displacement of the upper surface of the lower layer u_2, the transverse displacement of the upper layer v_{34}, the tangential displacement of the lower surface of the upper layer u_3, the tangential displacement of the upper surface of the upper layer u_4.

The finite element is constructed by summation from the previously described sub-elements by taking the correspondence and mutual equality of the degrees of freedom into account.

Numerical investigation of the wave motion

The composite shell of constant radius with the displacements of the first node equal to the displacements of the last node (periodic boundary conditions) is analyzed. The eighth eigenmode is shown in Fig. 1.

The ninth eigenmode is shown in Fig. 2. From the presented figures it is evident that the wave motion may be excited on those two multiple modes.

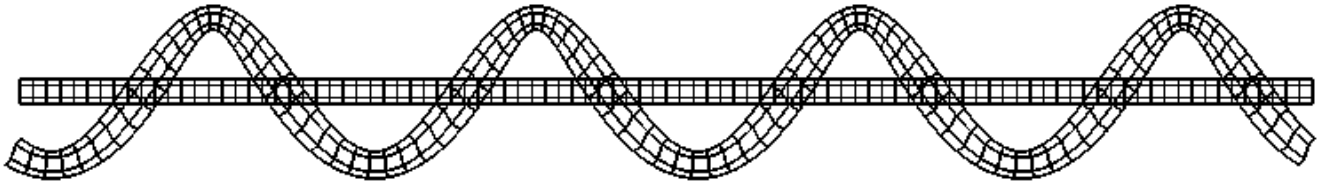

Fig. 1. **The structure in the status of equilibrium and the eighth eigenmode of the composite shell**

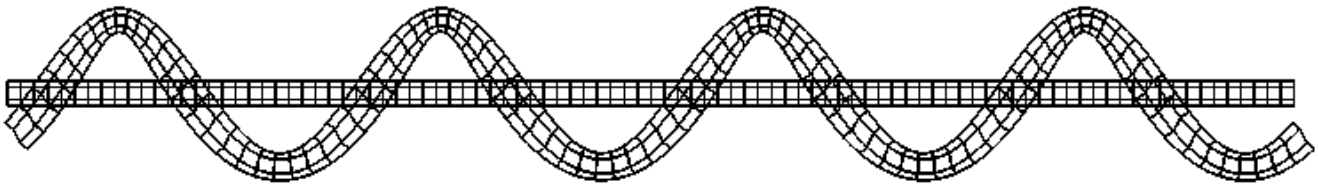

Fig. 2. **The structure in the status of equilibrium and the ninth eigenmode of the composite shell**

Transient processes of vibration supply of fluid

The orthogonal Cartesian coordinate system is defined where the z axis is parallel to the axis of the tube. It is assumed that the velocity of fluid flow in the direction of the flow is the function of the coordinates of the cross section and time, while the components of velocity in the plane of the cross section are given functions of time only, that is,

$$u=u(t),\ v=v(t),\ w=w(x,y,t), \quad (14)$$

where u, v, w denote the velocity components in the direction of the Cartesian orthogonal axes of coordinates, t is the time. It is assumed that the cross section of the tube does not vary with the z coordinate.

Thus the incompressibility condition of the flow is identically satisfied. In this case the stresses take the form:

$$\begin{aligned}&\sigma_x=\sigma_y=\sigma_z=-p,\\ &\sigma_{xy}=0,\\ &\sigma_{yz}=\mu w_y,\\ &\sigma_{zx}=\mu w_x,\end{aligned} \quad (15)$$

where p denotes the pressure, μ is the viscosity of the fluid, the subscripts denote partial derivatives.

The dynamic equilibrium equation in the direction of the z axis takes the form (taking into account the full derivative of w):

$$\begin{aligned}&(\mu w_x)_x + (\mu w_y)_y - p_z + \rho g = \\ &= \rho w_t + \rho u w_x + \rho v w_y,\end{aligned} \tag{16}$$

where ρ is the density of the fluid, g is the acceleration of gravity, p_z is the gradient of the pressure in the direction of the z axis.

It is assumed that the fluid is non-Newtonian and the viscosity is expressed like:

$$\mu = \mu_1 + \mu_2 \sqrt{w_x^2 + w_y^2}\,, \tag{17}$$

where μ_1 and μ_2 are constants.

The boundary condition takes into account the longitudinal vibration of the tube:

$$-\mu w n = \alpha(w - w^*), \tag{18}$$

where n is the outward normal vector to the boundary of the cross section of the flow, α is the coefficient of slippage (sliding friction between the fluid and the surface of the tube) and w^* is the velocity of the wall in the direction of the z axis. It is assumed that the boundary is a round circle and performs harmonic oscillations. The appropriate components of the vibration vector are expressed like:

$$\begin{aligned}u &= a\sin(\omega t),\\ v &= b\sin(\omega t),\\ w^* &= c\sin(\omega t),\end{aligned} \tag{19}$$

where a, b and c denote the amplitudes of oscillations and ω denotes the frequency of oscillations.

So the problem is described by Eq. 16 taking into account Eq. 17 and the boundary condition Eq. 18. μ_1, μ_2, $-p_z+\rho g$, ρ, α are constant quantities.

The following non-dimensional quantities are introduced:

$$\begin{aligned}&\hat{x} = \frac{x}{R}, \hat{y} = \frac{y}{R}, \hat{z} = \frac{z}{R}, \hat{u} = \frac{u}{W}, \hat{v} = \frac{v}{W},\\ &\hat{w} = \frac{w}{W}, \hat{w}^* = \frac{w^*}{W}, \hat{p} = \frac{p}{P}, \hat{t} = \frac{t}{T},\end{aligned} \tag{20}$$

where the top sign denotes the corresponding non-dimensional quantity, R is the radius of the tube, W is the characteristic velocity, P is the standard atmospheric pressure, $T = \frac{2\pi}{\omega}$ (this gives $\omega t = 2\pi\hat{t}$).

The equation of motion (Eq. 16) after taking into account Eq. 17 takes the following form:

$$\begin{aligned}&\rho w_t + \rho(u w_x + v w_y) - \mu_1(w_{xx} + w_{yy}) -\\ &- \mu_2((\sqrt{w_x^2 + w_y^2}\, w_x)_x +\\ &+ (\sqrt{w_x^2 + w_y^2}\, w_y)_y) = \rho g - p_z.\end{aligned} \tag{21}$$

In the non-dimensional form:

$$\begin{aligned}&\mathrm{Sh}\hat{w}_{\hat{t}} + \hat{u}\hat{w}_{\hat{x}} + \hat{v}\hat{w}_{\hat{y}} - \mathrm{Re}^{-1}(\hat{w}_{\hat{x}\hat{x}} + \hat{w}_{\hat{y}\hat{y}}) -\\ &- \mathrm{Rp}^{-1}((\sqrt{\hat{w}_{\hat{x}}^2 + \hat{w}_{\hat{y}}^2}\,\hat{w}_{\hat{x}})_{\hat{x}} +\\ &+ (\sqrt{\hat{w}_{\hat{x}}^2 + \hat{w}_{\hat{y}}^2}\,\hat{w}_{\hat{y}})_{\hat{y}}) = \mathrm{Fr}^{-1} - \mathrm{Eu}\hat{p}_{\hat{z}},\end{aligned} \tag{22}$$

where the Strouhal number is $\mathrm{Sh} = \frac{R}{TW}$; the Reynolds number $\mathrm{Re} = \frac{\rho W R}{\mu_1}$; the pseudo-Reynolds number $\mathrm{Rp} = \frac{\rho R^2}{\mu_2}$; the Froude number $\mathrm{Fr} = \frac{W^2}{gR}$; the Euler number $\mathrm{Eu} = \frac{P}{\rho W^2}$.

The boundary condition (Eq.18) after taking into account Eq. 17 takes the following form:

$$\begin{aligned}&-\mu_1(w_x n_x + w_y n_y) - \mu_2\sqrt{w_x^2 + w_y^2}\,(w_x n_x +\\ &+ w_y n_y) = \alpha(w - w^*),\end{aligned} \tag{23}$$

where n_x and n_y are the direction cosines of the outward normal of the boundary of the cross-section of the tube. In non-dimensional form:

$$\begin{aligned}&-\mathrm{Re}^{-1}(\hat{w}_{\hat{x}} n_x + \hat{w}_{\hat{y}} n_y) -\\ &-\mathrm{Rp}^{-1}\sqrt{\hat{w}_{\hat{x}}^2 + \hat{w}_{\hat{y}}^2}\,(\hat{w}_{\hat{x}} n_x + \hat{w}_{\hat{y}} n_y) =\\ &= \mathrm{Sl}(\hat{w} - \hat{w}^*),\end{aligned} \tag{24}$$

where the slippage number is $\mathrm{Sl} = \frac{\alpha}{\rho W}$.

First a finite element formulation of this problem is developed which gives the first order matrix differential equation. The cross section of the flow is meshed using the finite element approximation. The resulting matrix differential equation

$$[C]\{\dot{\delta}\} + [K]\{\delta\} = \{F\}, \tag{25}$$

is obtained on the basis of the Galerkin method of weighted residuals [13] and the FEM matrixes take the form:

$$\begin{aligned}&[C] = \iint [N]^T \rho [N] dxdy,\\ &[K] = \iint [B]^T \mu_1 [B] dxdy + \oint [M]^T \alpha [M] ds,\\ &\{F\} = \iint [N]^T (\rho g - p_z) dxdy -\\ &- \iint [B]^T \mu_2 \sqrt{w_x^2 + w_y^2}\,[B]\{\delta\} dxdy -\\ &- \iint [N]^T \rho [u; v][B]\{\delta\} dxdy + \oint [M]^T \alpha w^* ds,\end{aligned} \tag{26}$$

where $\{\delta\}$ is the vector of nodal velocities. The upper dot in Eq. 25 denotes differentiation with respect to time; s is the boundary line of the cross section of the flow

$$[N]=[N_1 \quad N_2 \quad \cdots \quad N_n],$$
$$[B]=\begin{bmatrix} \frac{\partial N_1}{\partial x} & \frac{\partial N_2}{\partial x} & \cdots & \frac{\partial N_n}{\partial x} \\ \frac{\partial N_1}{\partial y} & \frac{\partial N_2}{\partial y} & \cdots & \frac{\partial N_n}{\partial y} \end{bmatrix}, \qquad (27)$$
$$[M]=[M_1 \quad M_2 \quad \cdots \quad M_m],$$

where N_1, N_2 ... are the shape functions of the finite element in the cross section of the flow, M_1, M_2 ... are the shape functions of the finite element on the boundary of the cross section of the flow. Also in the expression of $\{F\}$ in Eq. 26 w_x and w_y are determined from:

$$\begin{Bmatrix} w_x \\ w_y \end{Bmatrix}=[B]\{\delta\}. \qquad (28)$$

The vector $\{\delta\}$ in the expression of $\{F\}$ in Eq. 26 and in Eq. 28 is taken from the previous time step while numerically integrating the matrix differential equations.

The first eigenpairs of the homogeneous system following from Eq. 25 are determined. Zero initial conditions are assumed. Numerical integration of the one-dimensional modal equations is performed by the constant average velocity integration scheme of the Newmark type.

Finally, the mass flow rate is found by integrating over the cross sectional area:

$$Q=\iint \rho w(x,y)dxdy, \qquad (29)$$

where *w(x,y)* are the transverse velocities. They are calculated from $\{\delta\}$ by using the shape functions of the appropriate finite elements.

By introducing the non-dimensional quantity:

$$\hat{Q}=\frac{Q}{Q_s}, \qquad (30)$$

where Q_s denotes the standard mass flow rate, Eq. 29 is represented in the non-dimensional form:

$$\hat{Q}=\mathrm{Fl}\iint \hat{w}(\hat{x},\hat{y})d\hat{x}d\hat{y}, \qquad (31)$$

where the flow number is $\mathrm{Fl}=\frac{\rho W R^2}{Q_s}$.

The cross-section of the tube is assumed to be a circle. One fourth of the circular region is analyzed by taking the symmetries with respect to the axes of coordinates into account. The characteristics of the non-Newtonian fluid are assumed to represent a liquid type suspension:

$$\mu_1=.004\frac{g}{mms}=4cP, \mu_2=-.0001\frac{g}{mm}, \alpha=.04\frac{g}{mm^2 s},$$
$$\rho=.001\frac{g}{mm^3}, -p_z+\rho g=.003\frac{g}{mm^2 s^2}.$$

Radius of the tube R = 10 mm. Also a = b = 0 mm; c=8 mm; ω = 2 *rad/s*.

Numerical integration of the finite element equations shows the effect of increase of average mass flow rate due to vibrations (Fig. 3).

For another problem the characteristics of the fluid are assumed to represent a liquid type suspension:

$$\mu_1=.004\frac{g}{mms}=4cP, \mu_2=0\frac{g}{mm}, \alpha=.04\frac{g}{mm^2 s},$$
$$\rho=.001\frac{g}{mm^3}, -p_z+\rho g=.003\frac{g}{mm^2 s^2}.$$

Radius of the tube R = 10 mm. The excitation is assumed in the direction of the x axis (a=6 mm; b= c =0 mm; ω=2 *rad/s*).

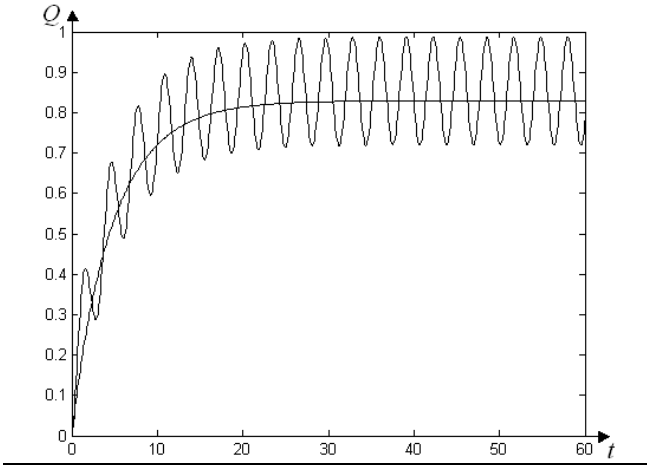

Fig.3. **Mass flow rate (g/s) without vibration excitation and with vibration excitation**

Numerical integration of the finite element equations shows the effect of decrease of the mass flow rate due to the vibrations of the tube (Fig. 4).

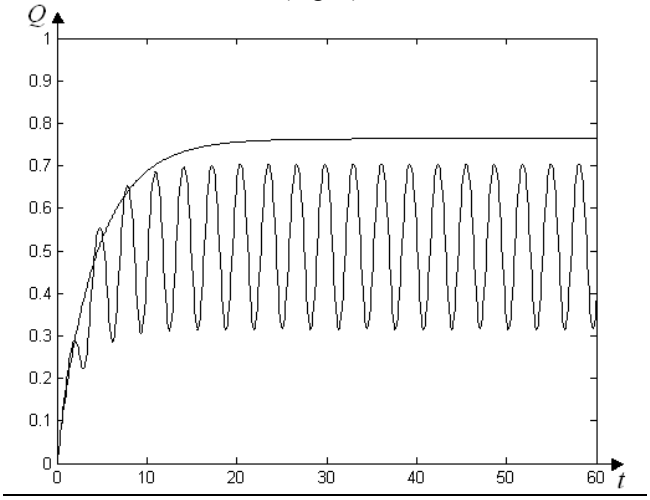

Fig.4. **Mass flow rate (g/s) without vibration excitation and with vibration excitation**

Photo-elastic investigation of viscous fluid flow

Fluid flow problems are studied by utilizing the effect of flow birefringence. Two dimensional laminar flow is analyzed. Birefringence is related to the deformation of ordinarily optically isotropic particles or is caused by the orientation of geometrically and optically an-isotropic particles. In both cases birefringence is related to the shear strain rate. Birefringence is taken as the integrated value through the light path. Boundary effects of the walls perpendicular to the light beam are not evaluated. The suspension used for photo-elastic investigations exhibits

non-Newtonian flow characteristics so it is desirable to perform the analysis in the low shear rate quasi-Newtonian region at low Reynolds numbers.

The velocities of the fluid are calculated by using the conventional formulation common in the finite element analysis [3]. The strain rates at the points of numerical integration of the finite element are calculated in the usual way [3]:

$$\begin{Bmatrix} \varepsilon_x \\ \varepsilon_y \\ \gamma_{xy} \end{Bmatrix} = [B]\{\delta_0\}, \tag{32}$$

where $\{\delta_0\}$ is the vector of nodal velocities; $[B]$ is the matrix relating the strain rates with the nodal velocities; ε_x, ε_y, γ_{xy} are the components of the strain rates. The velocities are continuous at inter-element boundaries, but the calculated strain rates are discontinuous due to the operation of differentiation.

The following systems of linear algebraic equations for the determination of each of the components of the strain rates using the conjugate approximation [15] are to be solved:

$$\begin{aligned} \iint [N]^T [N] dxdy \cdot \{\delta_x\} &= \iint [N]^T \varepsilon_x dxdy, \\ \iint [N]^T [N] dxdy \cdot \{\delta_y\} &= \iint [N]^T \varepsilon_y dxdy, \\ \iint [N]^T [N] dxdy \cdot \{\delta_{xy}\} &= \iint [N]^T \gamma_{xy} dxdy, \end{aligned} \tag{33}$$

where $\{\delta_x\}$ is the global vector of nodal values of ε_x; $\{\delta_y\}$ is the global vector of nodal values of ε_y; $\{\delta_{xy}\}$ is the global vector of nodal values of γ_{xy}; $[N]$ is the row of the shape functions of the finite element. The integration operators include integration over the elements and the direct stiffness procedure.

In order to obtain sufficiently smooth results the components of the strain rates are expanded using the first eigenmodes of the supplementary problem. This problem is the eigenproblem for the two-dimensional wave equation. The first eigenmodes of this problem are denoted as $\{\delta_1\}, \{\delta_2\}, \ldots$ and their matrix is:

$$[\Delta] = [\{\delta_1\}\{\delta_2\}\ldots]. \tag{34}$$

The coefficients of expansion $\{z\}$ of a component of the strain rate with the nodal values $\{\delta\}$ are obtained from:

$$[\Delta]^T [M]\{\delta\} = \{z\}, \tag{35}$$

where $[M]$ is the mass matrix of the supplementary problem. In our case we have:

$$\begin{aligned} &[\Delta]^T \int [N]^T \begin{bmatrix} \varepsilon_x & \varepsilon_y & \gamma_{xy} \end{bmatrix} dxdy = \\ &= \begin{bmatrix} \{z_x\} & \{z_y\} & \{z_{xy}\} \end{bmatrix}, \end{aligned} \tag{36}$$

where $\{z_x\}$ are the coefficients of expansion of ε_x; $\{z_y\}$ are the coefficients of expansion of ε_y; $\{z_{xy}\}$ are the coefficients of expansion of γ_{xy}.

In the photo-elastic image the intensity is proportional to the intensity of the shear strain rate:

$$\sqrt{\frac{1}{2}(\varepsilon_x - \varepsilon_y)^2 + \frac{1}{2}\varepsilon_x^2 + \frac{1}{2}\varepsilon_y^2 + \frac{3}{4}\gamma_{xy}^2}\ . \tag{37}$$

The rectangular region with the components of the velocities prescribed on the boundaries is analyzed. The prescribed velocities on the boundaries are everywhere zero, except the velocities in the direction of the *y* axis at the nodes in the middle of the lower and upper boundaries, where they are assumed to be equal to one. The reconstructed photo-elastic image by using 8 eigenmodes of the supplementary problem and represented by the intensity mapping proposed in [16] is shown in Fig. 5.

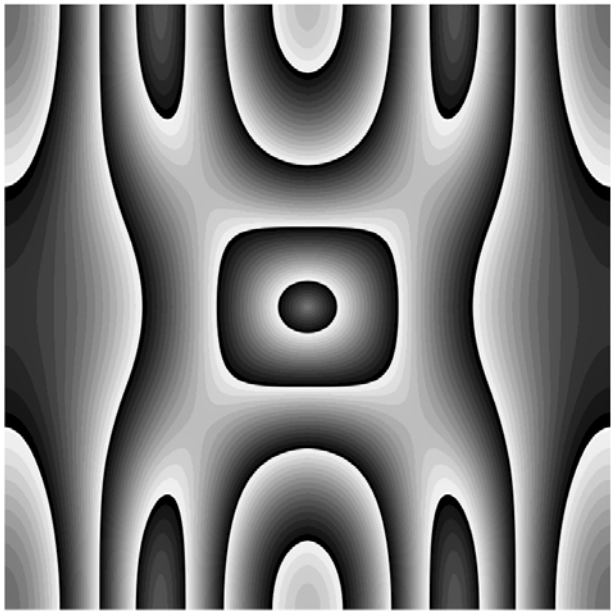

Fig. 5**. Photo-elastic image represented by intensity mapping**

In this problem concentration of the strain rate at the loading points takes place. The mesh is too coarse to represent the results there. The proposed eigen-smoothing procedure produces interpretable results according to which qualitative correspondence with the photo-elastic experiment may be expected.

Conclusions

The finite element of the axi-symmetric composite shell problem is constructed. It is shown that the multiple eigenmodes exist in an analyzed periodic system. They are suitable for the excitation of wave motion in it.

The mathematical model describing the motion of fluid in a tube performing vibrations is developed. The velocity of the longitudinal motion of the walls is taken into account through the boundary condition. Transverse motions are incorporated through the convective inertia terms. The results of the analysis show that the transverse vibrations decrease the mass flow rate, while the longitudinal vibrations increase it. Thus the change of the mass flow rate caused by one of the types of vibrations can be compensated by the vibrations of another type.

For the analysis of viscous fluid flow the velocity based formulation is coupled with the photo-elastic analysis based on the intensity of the shear strain rate. The procedure of conjugate approximation with eigen-

smoothing enables generation of photo-elastic images with acceptable quality.

References

1. **Ragulskienė J., Maciulevičius J., Maskeliūnas R., Zubavičius L.** Investigation of the oscillatory dynamics of the interacting plates. 2003. Ultragarsas, Nr. 4(49). P. 24-26.
2. **Obrazcov I. F., Savieljiev L. M., Hazanov H. S.** The method of finite elements in the problems of building mechanics of flying devices. Moscow: Vysshaja shkola. 1985. P. 392.
3. **Bathe K.-J.** Finite element procedures in engineering analysis. New Jersey: Prentice-Hall. 1982. P. 738.
4. **Baker A. J.** Finite Element Computational Fluid Mechanics. Hemisphere PC, USA., 1983. P. 510.
5. **Blawzdziewicz J., Feuillebois F**. Calculation of an Effective Slip in a Settling Suspension at a Vertical Wall. International Journal of Fluid Mechanics Research. 1995. Vol.22. No.1. P. 164–169.
6. **Bubulis A., Ragulskis L.** Dry Substances Transportation and Dosing Using Vibrations. 41 Internationales Wissenchaftliches Kolloquium, Ilmenau. 1996. P. 492 –496.
7. **Hauser G., Sommer K.** Plug flow type pneumatic conveying of abrasive products in food industry, Journal of Powder & Bulk Solids Technology. 1998. No.12. P. 511-519.
8. **Huang Y., Hsu C.** Dynamic Behaviour of Tubes Subjected to Internal and External Cross Flows. J. Shock and Vibration. 1997. Vol. 4. No.2. P. 77-91.
9. **Hui L., Tomita Y.** A numerical simulation of swirling flow pneumatic conveying in a horizontal pipeline. Particulate Science and Technology: An International Journal. 2000. Vol.18(4). P. 275-292.
10. **Jacobsen M. L., McCluskey D. R., Easson W. J., Greated C. A.** Pneumatic particle conveyance in a pipe bend: simultaneous two phase PIV measurements of the slip velocity between the air and particle phases. 7-th Int. Symposium on Applications of Laser Techniques to Fluid Mechanics. Lisbon, 1994.
11. **Morgan K., Peraire J.** Unstructured Grid Finite Element Methods for Fluid Dynamics. Reports on Progress in Physics. Institute of Physics, USA. 1998. Vol.61. No.6. P. 569–638.
12. **Ragulskis M., Palevicius A.** Theoretical and Experimental Studies of Tubular Valve Dynamics. International Journal of Acoustics and Vibration. 2002. Vol. 7. No. 1. P. 53-57.
13. **Rao. S. S.** The Finite Element Method in Engineering. Pergamon Press, U.K. 1982. P. 625.
14. **Thomasset F.** Implementation of Finite Element Methods for Navier-Stokes Equations. Springer Verlag, Germany. 1981. P. 159.
15. **Segerlind L. J.** Applied Finite Element Analysis. Moscow: Mir. 1979. P. 392.
16. **Ragulskis M., Kravčenkienė V.** Investigation of the oscillatory dynamics of the plate with the control layer of material. 2003. Ultragarsas. Nr.1(46). P. 20-23.

K. Ragulskis, E. Kibirkštis, A. Bubulis, L. Zubavičius, R. Maskeliūnas, L. Ragulskis

Spausdinimo įtaiso elementų dinamika

Reziumė

Ašiasimetrio sudėtinio kevalo uždavinio baigtinis elementas sudarytas iš sluoksnių subelementų. Periodinės konstrukcijos savosios formos tinkamos banginiam judesiui žadinti.

Sudarytas skysčio judesio virpamąjame vamzdyje skaitmeninis modelis. Analizės rezultatai parodo, kad skersiniai virpesiai mažina pratekančio skysčio kiekį, o išilginiai didina. Todėl vieno tipo virpesių sukeltas skysčio srauto pasikeitimas gali būti kompensuotas kito tipo virpesiais.

Klampaus skysčio tekėjimo analizėje kaip mazginiai kintamieji imami greičiai. Fototampriems vaizdams, besiremiantiems deformacijų greičiais, gauti pasiūlyta glotninimo metodika.

Pateikta spaudai 2004 03